Available online at www.sciencedirect.com
ScienceDirect
Computer Physics Communications 177 (2007) 566–583
Computer Physics Communications
www.elsevier.com/locate/cpc

Symplectic and multi-symplectic methods for coupled nonlinear Schrödinger equations with periodic solutions

A. Aydın [a], B. Karasözen [b,*]

[a] *Department of Mathematics, Atılım University, 06836 Ankara, Turkey*
[b] *Department of Mathematics and Institute of Applied Mathematics, Middle East Technical University, 06531 Ankara, Turkey*

Received 20 July 2006; received in revised form 18 May 2007; accepted 22 May 2007

Available online 5 June 2007

Abstract

We consider for the integration of coupled nonlinear Schrödinger equations with periodic plane wave solutions a splitting method from the class of symplectic integrators and the multi-symplectic six-point scheme which is equivalent to the Preissman scheme. The numerical experiments show that both methods preserve very well the mass, energy and momentum in long-time evolution. The local errors in the energy are computed according to the discretizations in time and space for both methods. Due to its local nature, the multi-symplectic six-point scheme preserves the local invariants more accurately than the symplectic splitting method, but the global errors for conservation laws are almost the same.

PACS: 02.70.Bf; 42.65.Sf

Keywords: Coupled nonlinear Schrödinger equation; Periodic waves; Symplectic and multi-symplectic methods; Splitting

1. Introduction

The nonlinear Schrödinger equation (NLS) arises as model equation with second-order dispersion and cubic nonlinearity for describing the dynamics of slowly varying wave packets in nonlinear optics and fluid dynamics. If there are two or more modes the coupled nonlinear Schrödinger (CNLS) system would be the relevant model. The two coupled nonlinear Schrödinger (CNLS) equations are given by

$$\begin{aligned} i\frac{\partial\psi_1}{\partial t}+\alpha_1\frac{\partial^2\psi_1}{\partial x^2}+\left(\sigma_1|\psi_1|^2+v_{12}|\psi_2|^2\right)\psi_1=0,\\ i\frac{\partial\psi_2}{\partial t}+\alpha_2\frac{\partial^2\psi_2}{\partial x^2}+\left(\sigma_2|\psi_2|^2+v_{21}|\psi_1|^2\right)\psi_2=0, \end{aligned} \tag{1}$$

where $\psi_1(x,t)$ and $\psi_2(x,t)$ are complex amplitudes or 'envelopes' of two wave packets, i is the imaginary number, x and t are the space and time variables, respectively. The CNLS system has many applications including nonlinear optics [1,2] and geophysical fluid dynamics [3,4]. The parameters α_j are the dispersion coefficients, σ_j the Landau constants which describe the self-modulation of the wave packets, and v_{12} and v_{21} are the wave–wave interaction coefficients which describe the cross-modulations of the wave packets [5,6].

Analytical solutions can be obtained only for a few special integrable cases, like the Manakov model [1] where the self-modulation and wave–wave interaction coefficients are equal, i.e. $\alpha_1=\alpha_2=1$, $\sigma_1=\sigma_2=v_{12}=v_{21}$. Other integrable cases are: $\alpha_1=\alpha_2$, $\sigma_1=\sigma_2=v_{12}=v_{21}$ and $\alpha_1=-\alpha_2$, $\sigma_1=\sigma_2=-v_{12}=-v_{21}$ which can be solved by the inverse scattering method [7].

* Corresponding author.
E-mail address: bulent@metu.edu.tr (B. Karasözen).

0010-4655/$ – see front matter
doi:10.1016/j.cpc.2007.05.010

For nonintegrable cases, where the parameters are different, numerical methods have to be used in order to understand different nonlinear phenomena that arise by the interaction of stable and unstable wave packets in the CNLS system.

There has been a lot work done for the solitary wave solutions of (1). Symplectic and multi-symplectic methods are also used for the numerical solution of soliton collision [8,9]. Little attention has been paid to plane wave solutions under periodic boundary conditions. In this work we will consider the plane wave solutions of (1) under periodic boundary conditions with period L

$$\psi_1(x,t) = \psi_{10} e^{i(k_1 x - \omega_1 t)}, \qquad \psi_t(x,t) = \psi_{20} e^{i(k_2 x - \omega_2 t)}$$

with the dispersion relations

$$\omega_1 = \alpha_1 k_1^2 - \left(\sigma_1 a_1^2 + v_{12} a_2^2\right), \qquad \omega_2 = \alpha_2 k_1^2 - \left(\sigma_2 a_1^2 + v_{21} a_2^2\right),$$

where the amplitudes ψ_{10} and ψ_{20} are assumed to be real [5,6]. We take $v_{12} = v_{21} = v$ because this choice of the parameters allows a multi-symplectic formulation of the CNLS system.

Besides the Manakov's case which corresponds to elliptical polarization we consider two other polarizations [5,6]:

- linear polarization: $v_{12} = v_{21} = 2/3$,
- circular polarization: $v_{12} = v_{21} = 2$

with $\alpha_1 = \alpha_2 = 1$, $\sigma_1 = \sigma_2 = 1$.

Several numerical studies have been carried out in recent years in order to understand the behavior of the periodic plane wave solutions of the CNLS system. In [5] a pseudospectral discretization was used in the space variables and the resulting system of ordinary differential equations (ODEs) were integrated using the standard fourth-order Runge–Kutta method. Because the method used in [5] is not conservative, no indication is given about the preservation of the conserved quantities of the CNLS system. In [6] the CNLS system with periodic boundary conditions was discretized in space using second-order finite differences and the resulting system of ordinary differential equations (ODEs) are integrated in time using the so-called Hopscotch method, a mixture of an explicit and an implicit method. The accuracy of the solutions were checked only using the norm conservation of each amplitude of the CNLS system. The choice of particular initial conditions may affect the preservation of some invariants. As mentioned in [10] in the context of multi-symplectic integrators usually symmetric initial conditions are used in the literature. Unsymmetric initial conditions may lead to an increase of errors in preserving some invariants like momentum over time [10].

The numerical solution of nonlinear wave equations using symplectic and multi-symplectic geometric integrators has been the subject of many studies in recent years (see for a recent review [11]). The NLS and CNLS systems represent an infinite-dimensional Hamiltonian system. After semi-discretization in the space variables one usually obtains a system of Hamiltonian ordinary differential equations, for which various symplectic integrators can be applied [8,12,13]. In Section 2 we give a symplectic integrator based on the splitting of the semi-discretized Hamiltonian system in linear and nonlinear parts. Another way is to use the multi-symplectic structure of the NLS and CNLS equations and apply multi-symplectic integrators [9,14,15]. A brief review of multi-symplectic integrators and their application to the CNLS system given in Section 3. In Section 4 numerical results obtained with the symplectic splitting method and multi-symplectic six-point Preissman scheme are compared with results found in the literature for symmetric and unsymmetric initial conditions. Section 5 is devoted to concluding remarks.

2. Symplectic splitting method

PDEs are usually discretized first in space resulting in a large system of ODEs. The resulting system of ODEs is then integrated by an appropriate time-stepping method. Infinite-dimensional Hamiltonian systems can be also discretized by ensuring that the resulting finite-dimensional system is also Hamiltonian. The infinite-dimensional Hamiltonian system can be discretized in space either starting from the Lagrangian functional or from the Hamiltonian functional with the Poisson bracket. Here we apply the second approach. A summary of semi-discretization methods for Hamiltonian systems is given in [11,16].

By decomposing the complex functions ψ_1, ψ_2 of (1) into real and imaginary parts

$$\psi_1(x,t) = q_1(x,t) + i q_2(x,t), \qquad \psi_2(x,t) = q_3(x,t) + i q_4(x,t)$$

the CNLS systems (1) can be written as a system of real-valued equations

$$\begin{aligned}
&\frac{\partial q_1}{\partial t} + \alpha_1 \frac{\partial^2 q_2}{\partial x^2} + \left(\sigma_1\left(q_1^2 + q_2^2\right) + v\left(q_3^2 + q_4^2\right)\right) q_2 = 0,\\
&\frac{\partial q_2}{\partial t} - \alpha_1 \frac{\partial^2 q_1}{\partial x^2} - \left(\sigma_1\left(q_1^2 + q_2^2\right) + v\left(q_3^2 + q_4^2\right)\right) q_1 = 0,\\
&\frac{\partial q_3}{\partial t} + \alpha_2 \frac{\partial^2 q_4}{\partial x^2} + \left(v\left(q_1^2 + q_2^2\right) + \sigma_2\left(q_3^2 + q_4^2\right)\right) q_4 = 0,
\end{aligned}$$

$$\frac{\partial q_4}{\partial t} - \alpha_2 \frac{\partial^2 q_3}{\partial x^2} - \big(v\big(q_1^2 + q_2^2\big) + \sigma_2\big(q_3^2 + q_4^2\big)\big)q_3 = 0. \tag{2}$$

These equations represent an infinite-dimensional Hamiltonian system in the phase space $z = (q_1, q_2, q_3, q_4)^{\mathrm{T}}$

$$z_t = \mathbf{J}^{-1}\frac{\delta \mathcal{H}}{\delta z}, \qquad \mathbf{J} = \begin{pmatrix} 0 & -1 & 0 & 0 \\ 1 & 0 & 0 & 0 \\ 0 & 0 & 0 & -1 \\ 0 & 0 & 1 & 0 \end{pmatrix}, \tag{3}$$

where the Hamiltonian is

$$\mathcal{H}(z) = \int \left\{ \mathcal{W} - \frac{\alpha_1}{2}\left(\left(\frac{\partial q_1}{\partial x}\right)^2 + \left(\frac{\partial q_2}{\partial x}\right)^2\right) - \frac{\alpha_2}{2}\left(\left(\frac{\partial q_3}{\partial x}\right)^2 + \left(\frac{\partial q_4}{\partial x}\right)^2\right)\right\} \mathrm{d}x, \tag{4}$$

with $\mathcal{W} = \frac{1}{4}(\sigma_1(q_1^2 + q_2^2)^2 + \sigma_2(q_3^2 + q_4^2)^2) + \frac{v}{2}(q_1^2 + q_2^2)(q_3^2 + q_4^2)$.

An efficient way of time discretization of semi-discretized PDEs in symplectic form is by splitting. The basic idea of splitting is to decompose the original problem into subproblems which are easier to solve then recompose them. Splitting can be performed either on the Hamiltonian or on the vector field. Splitting techniques which are originally developed for multi-dimensional PDEs have been successfully applied to geometric integrators (for a review see [17], Chapter II and [18]). If each vector field resulting from the splitting happens to be integrable for the solution of ODEs, then a numerical integration scheme is obtained as the concatenation of the flows of the individual subsystems. However the splitting depends on the particular problem. For nonlinear wave equations like shallow water equations, the Boussinesq equation and the KdV equation different splitting are used for the space variables in [19]. For the generalized nonlinear Schrödinger equation a linear–nonlinear splitting was used in [20] and the resulting system of ODEs is integrated in time by a symplectic composition method.

In [8] the space variables were discretized by a second-order central difference operator and was shown that the resulting semi-discretization is a Hamiltonian system for a CNLS system. The time derivative was discretized by the implicit midpoint rule and constructed a symplectic integrator of the CNLS system. After elimination of some variables, a symplectic six-point scheme was obtained. The symplectic six-point scheme was tested for the evolution of the solitary waves of the CNLS system. It was shown that the symplectic six-point scheme preserves the discrete analog of the mass conservation exactly.

In this section a semi-implicit symplectic scheme for the CNLS equation will be derived by splitting the vector field (2) into linear and nonlinear parts. The linear vector field for (2) can be written as

$$\begin{aligned} \frac{\partial q_1}{\partial t} &= -\alpha_1 \frac{\partial^2 q_2}{\partial x^2}, & \frac{\partial q_2}{\partial t} &= \alpha_1 \frac{\partial^2 q_1}{\partial x^2}, \\ \frac{\partial q_3}{\partial t} &= -\alpha_2 \frac{\partial^2 q_4}{\partial x^2}, & \frac{\partial q_4}{\partial t} &= \alpha_2 \frac{\partial^2 q_3}{\partial x^2} \end{aligned} \tag{5}$$

and the nonlinear vector field for (2) can be written as

$$\begin{aligned} \frac{\partial q_1}{\partial t} &= -\big(\sigma_1\big(q_1^2 + q_2^2\big) + v\big(q_3^2 + q_4^2\big)\big)q_2, \\ \frac{\partial q_2}{\partial t} &= \big(\sigma_1\big(q_1^2 + q_2^2\big) + v\big(q_3^2 + q_4^2\big)\big)q_1, \\ \frac{\partial q_3}{\partial t} &= -\big(v\big(q_1^2 + q_2^2\big) + \sigma_2\big(q_3^2 + q_4^2\big)\big)q_4, \\ \frac{\partial q_4}{\partial t} &= \big(v\big(q_1^2 + q_2^2\big) + \sigma_2\big(q_3^2 + q_4^2\big)\big)q_3. \end{aligned} \tag{6}$$

Notice that the linear subproblem (5) and nonlinear subproblem (6) can be written as an infinite-dimensional Hamiltonian system (3) for $\mathcal{H}(z) = \mathcal{H}_{\mathrm{Lin}}$ and $\mathcal{H}(z) = \mathcal{H}_{\mathrm{Non}}$ with

$$\mathcal{H}_{\mathrm{Lin}} = -\int \left\{ \frac{\alpha_1}{2}\left(\left(\frac{\partial q_1}{\partial x}\right)^2 + \left(\frac{\partial q_2}{\partial x}\right)^2\right) + \frac{\alpha_2}{2}\left(\left(\frac{\partial q_3}{\partial x}\right)^2 + \left(\frac{\partial q_4}{\partial x}\right)^2\right)\right\} \mathrm{d}x, \tag{7}$$

and

$$\mathcal{H}_{\mathrm{Non}} = \int \left\{ \frac{1}{4}\big(\sigma_1\big(q_1^2 + q_2^2\big)^2 + \sigma_2\big(q_3^2 + q_4^2\big)^2\big) + \frac{v}{2}\big(q_1^2 + q_2^2\big)\big(q_3^2 + q_4^2\big)\right\} \mathrm{d}x. \tag{8}$$

Consequently, splitting the vector field (2) into linear subproblem (5) and nonlinear subproblem (6) corresponds to splitting the Hamiltonian (4) as $\mathcal{H} = \mathcal{H}_{\mathrm{Lin}} + \mathcal{H}_{\mathrm{Non}}$.

2.1. Hamiltonian discretization

Using a forward difference approximation for the first-order derivatives in the Hamiltonian (4), we obtain a finite-dimensional Hamiltonian system (see, for example, [19]). In (7) the first-order derivatives q_{i_x}, $i = 1, \ldots, 4$, are discretized using the mesh points x_m, x_{m+1}. The space mesh size will be denoted by $\Delta x = x_{m+1} - x_m$ with $\Delta x = L/N$, where N is the number of mesh points. For simplicity, we will use the notation $q_{i_m} = q_i(mL/N, t)$, as finite difference approximations to the exact solutions q_i at the mesh points. The discretized Hamiltonian (4) is then

$$\begin{aligned} H_{\Delta x} = {} & \Delta x \sum_{m=1}^{N} \left[\frac{1}{4} \left(\sigma_1 \left(q_{1_m}^2 + q_{2_m}^2 \right)^2 + \sigma_2 \left(q_{3_m}^2 + q_{4_m}^2 \right)^2 \right) + V(q_m) \right] \\ & - \Delta x \sum_{m=1}^{N} \frac{\alpha_1}{2} \left[\left(\frac{q_{1_{m+1}} - q_{1_m}}{\Delta x} \right)^2 + \left(\frac{q_{2_{m+1}} - q_{2_m}}{\Delta x} \right)^2 \right] \\ & - \Delta x \sum_{m=1}^{N} \frac{\alpha_2}{2} \left[\left(\frac{q_{3_{m+1}} - q_{3_m}}{\Delta x} \right)^2 + \left(\frac{q_{4_{m+1}} - q_{4_m}}{\Delta x} \right)^2 \right], \end{aligned} \tag{9}$$

where $V(q_m) := \frac{1}{2} v (q_{1_m}^2 + q_{2_m}^2)(q_{3_m}^2 + q_{4_m}^2)$.

2.2. Splitting

The Hamiltonian $H_{\Delta x}$ can be split into linear and nonlinear parts:

$$\begin{aligned} H_{\text{lin}} = {} & -\Delta x \sum_{m=1}^{N} \frac{\alpha_1}{2} \left[\left(\frac{q_{1_{m+1}} - q_{1_m}}{\Delta x} \right)^2 + \left(\frac{q_{2_{m+1}} - q_{2_m}}{\Delta x} \right)^2 \right] \\ & - \Delta x \sum_{m=1}^{N} \frac{\alpha_2}{2} \left[\left(\frac{q_{3_{m+1}} - q_{3_m}}{\Delta x} \right)^2 + \left(\frac{q_{4_{m+1}} - q_{4_m}}{\Delta x} \right)^2 \right], \end{aligned} \tag{10}$$

$$H_{\text{non}} = \Delta x \sum_{m=1}^{N} \left[\frac{1}{4} \left(\sigma_1 \left(q_{1_m}^2 + q_{2_m}^2 \right)^2 + \sigma_2 \left(q_{3_m}^2 + q_{4_m}^2 \right)^2 \right) + V(q_m) \right]. \tag{11}$$

We notice that (10) corresponds to the discretization of (7) and (11) corresponds to the discretization of (8).

A standard discretization of the linear subproblem (5) by means of the method of lines consists of discretization first in space and then in time. After the discretization in space using the central difference approximation for the second-order derivatives, we get the semi-discretized linear subproblem

$$\begin{aligned} \frac{\mathrm{d}q_{1_m}}{\mathrm{d}t} &= -\alpha_1 \frac{q_{2_{m-1}} - 2q_{2_m} + q_{2_{m+1}}}{2\Delta x^2}, & \frac{\mathrm{d}q_{2_m}}{\mathrm{d}t} &= \alpha_1 \frac{q_{1_{m-1}} - 2q_{1_m} + q_{1_{m+1}}}{2\Delta x^2}, \\ \frac{\mathrm{d}q_{3_m}}{\mathrm{d}t} &= -\alpha_2 \frac{q_{4_{m-1}} - 2q_{4_m} + q_{4_{m+1}}}{2\Delta x^2}, & \frac{\mathrm{d}q_{4_m}}{\mathrm{d}t} &= \alpha_2 \frac{q_{3_{m-1}} - 2q_{3_m} + q_{3_{m+1}}}{2\Delta x^2}. \end{aligned} \tag{12}$$

This system of ODEs can be formulated as a finite-dimensional Hamiltonian system with linear and nonlinear parts. The linear part is given as

$$\frac{\mathrm{d}Z}{\mathrm{d}t} = J^{-1} \nabla H_{\text{lin}}(Z), \quad \text{with } Z := (Q_1, Q_2, Q_3, Q_4)^{\mathrm{T}}, \tag{13}$$

where $Q_i := (q_{i_1}, q_{i_2}, \ldots, q_{i_N})$, $i = 1, \ldots, 4$, and

$$J := \begin{pmatrix} 0 & -I & 0 & 0 \\ I & 0 & 0 & 0 \\ 0 & 0 & 0 & -I \\ 0 & 0 & I & 0 \end{pmatrix}.$$

The semi-discretized nonlinear subproblem for (6) is

$$\begin{aligned} \frac{\partial q_{1_m}}{\partial t} &= -\left[\sigma_1 \left(q_{1_m}^2 + q_{2_m}^2 \right) + v \left(q_{3_m}^2 + q_{4_m}^2 \right) \right] q_{2_m}, \\ \frac{\partial q_{2_m}}{\partial t} &= \left[\sigma_1 \left(q_{1_m}^2 + q_{2_m}^2 \right) + v \left(q_{3_m}^2 + q_{4_m}^2 \right) \right] q_{1_m}, \end{aligned}$$

$$\frac{\partial q_{3_m}}{\partial t} = -\left[v\left(q_{1_m}^2 + q_{2_m}^2\right) + \sigma_2\left(q_{3_m}^2 + q_{4_m}^2\right)\right] q_{4_m},$$
$$\frac{\partial q_{4_m}}{\partial t} = \left[v\left(q_{1_m}^2 + q_{2_m}^2\right) + \sigma_2\left(q_{3_m}^2 + q_{4_m}^2\right)\right] q_{3_m}. \tag{14}$$

The systems (13) and (14) are solved by the symplectic implicit mid-point rule. After applying the implicit mid-point rule to the linear part (13)

$$\frac{Z^{n+1} - Z^n}{\Delta t} = J^{-1} \nabla H_{\text{lin}}\left(\frac{Z^{n+1} + Z^n}{2}\right), \tag{15}$$

the discrete system of linear equations can be written as

$$\begin{pmatrix} I & A_1 & 0 & 0 \\ -A_1 & I & 0 & 0 \\ 0 & 0 & I & A_2 \\ 0 & 0 & -A_2 & I \end{pmatrix} \begin{pmatrix} Q_1^{n+1} \\ Q_2^{n+1} \\ Q_3^{n+1} \\ Q_4^{n+1} \end{pmatrix} = \begin{pmatrix} I & -A_1 & 0 & 0 \\ A_1 & I & 0 & 0 \\ 0 & 0 & I & -A_2 \\ 0 & 0 & A_2 & I \end{pmatrix} \begin{pmatrix} Q_1^{n} \\ Q_2^{n} \\ Q_3^{n} \\ Q_4^{n} \end{pmatrix}, \tag{16}$$

where

$$A_i = \alpha_i \frac{\Delta t}{2\Delta x^2} \begin{pmatrix} -2 & 1 & & & & 1 \\ 1 & -2 & 1 & & & \\ & & \ddots & & & \\ & & & 1 & -2 & 1 \\ 1 & & & & 1 & -2 \end{pmatrix}.$$

However, the nonlinear subsystem (14) requires a nonlinear solver for which we have used the simplified Newton method.

We notice that the semi-discretized system in space considering the formulas (12) and (14), is symmetric so that the results given in [10] for the single Schrödinger equation can be compared with ours.

2.3. Composition method

The idea of the composition method is based on either the splitting of the vector field of a differential equation $\mathrm{d}x/\mathrm{d}t = X(x)$ or the Hamiltonian. Then each X_j is integrated exactly or approximately. These solutions are composed in an appropriate way to obtain an integrator for the vector field $X(x)$. Since the vector fields X_j's are usually noncommutative, the composition yields an error. This splitting error can be analyzed by the Baker–Campbell–Haussdorff (BCH) formula (see Chapter III.5.3–4 in [17], and [18]).

The solutions of (13) and (14) by the mid-point rule can be composed by the second-order symmetric integrator [17,18,20]

$$\varphi_2(\Delta t) = e^{\frac{\Delta t}{2} H_{\text{non}}} \circ e^{\Delta t H_{\text{lin}}} \circ e^{\frac{\Delta t}{2} H_{\text{non}}} \tag{17}$$

which results a symplectic integrator for the CNLS system (1). Higher-order compositions can be obtained by suitable composition of the second-order integrator [17,18,20].

3. Multi-symplectic structure of coupled nonlinear Schrödinger equation

3.1. Multi-symplectic formulation of Hamiltonian PDEs and of the CNLS system

Multi-symplectic Hamiltonian PDEs can be written in canonical form

$$\mathbf{M} z_t + \mathbf{K} z_x = \nabla_z S(z), \quad z \in \mathbf{R}^n, \tag{18}$$

where $\mathbf{M}$ and $\mathbf{K}$ are skew-symmetric matrices on $\mathbf{R}^n$ ($n \geqslant 3$) and S is a smooth function of the state variable $z(x,t)$, and ∇_z denotes the gradient operator in $\mathbf{R}^n$ [11,15,21]. A system of the form (18) preserves symplectic structure in space and time

$$\omega_t + \kappa_x = 0 \quad \text{with } \omega := \frac{1}{2}\,\mathrm{d}z \wedge \mathbf{M}\,\mathrm{d}z, \quad \kappa := \frac{1}{2}\,\mathrm{d}z \wedge \mathbf{K}\,\mathrm{d}z, \tag{19}$$

where $\wedge$ denotes the wedge product.

When S is independent of x and t, the system (18) has local energy and momentum conservation laws

$$E_t + F_x = 0, \qquad E(z) = S(z) - \frac{1}{2} z^{\mathrm{T}} \mathbf{K} z_x, \qquad F(z) = \frac{1}{2} z^{\mathrm{T}} \mathbf{K} z_t,$$

$$I_t + G_x = 0, \qquad G(z) = S(z) - \frac{1}{2} z^{\mathrm{T}} \mathbf{M} z_t, \qquad I(z) = \frac{1}{2} z^{\mathrm{T}} \mathbf{M} z_x. \tag{20}$$

Introducing the canonical momenta p_j, $j = 1, \ldots, 4$,

$$p_1 + i p_2 = \alpha_1 \frac{\partial \psi_1}{\partial x}, \qquad p_3 + i p_4 = \alpha_2 \frac{\partial \psi_2}{\partial x}$$

or in explicit form:

$$p_1 = \alpha_1 \frac{\partial q_1}{\partial x}, \qquad p_2 = \alpha_1 \frac{\partial q_2}{\partial x}, \qquad p_3 = \alpha_2 \frac{\partial q_3}{\partial x}, \qquad p_4 = \alpha_2 \frac{\partial q_4}{\partial x}, \tag{21}$$

the CNLS system can now be formulated as a multi-symplectic form of type (18) with the state variable $z = (q_1, q_2, q_3, q_4, p_1, p_2, p_3, p_4)^{\mathrm{T}}$

$$\mathbf{M} = \begin{pmatrix} -J & 0 \\ 0 & 0 \end{pmatrix}, \qquad \mathbf{K} = \begin{pmatrix} 0 & -I \\ I & 0 \end{pmatrix}, \tag{22}$$

where

$$S(z) = W + \frac{1}{2\alpha_1}\left(p_1^2 + p_2^2\right) + \frac{1}{2\alpha_2}\left(p_3^2 + p_4^2\right)$$

with

$$W = \frac{\sigma_1}{4}\left(q_1^2 + q_2^2\right)^2 + \frac{\sigma_2}{4}\left(q_3^2 + q_4^2\right)^2 + \frac{v}{2}\left(q_1^2 + q_2^2\right)\left(q_3^2 + q_4^2\right), \tag{23}$$

J as defined in (3), 0, I denote the 4×4 zero and identity matrices, respectively. The local energy and momentum conservation laws (20) are given with

$$\begin{aligned}
E(z) &= W - \frac{1}{2\alpha_1}\left(p_1^2 + p_2^2\right) - \frac{1}{2\alpha_2}\left(p_3^2 + p_4^2\right), \\
F(z) &= p_1 \frac{\partial q_1}{\partial t} + p_2 \frac{\partial q_2}{\partial t} + p_3 \frac{\partial q_3}{\partial t} + p_4 \frac{\partial q_4}{\partial t}, \\
I(z) &= \frac{1}{2}\left(\frac{1}{\alpha_1}(q_1 p_2 - q_2 p_1) + \frac{1}{\alpha_2}(q_3 p_4 - q_4 p_3)\right), \\
G(z) &= S(z) - \frac{1}{2}\left(q_1 \frac{\partial q_2}{\partial t} - q_2 \frac{\partial q_1}{\partial t} + q_3 \frac{\partial q_4}{\partial t} - q_4 \frac{\partial q_3}{\partial t}\right),
\end{aligned} \tag{24}$$

where W is defined in (23). We have for the CNLS system additionally norm conservation which results from the phase invariance of the solutions [22]

$$N_t + M_x = 0, \qquad N = \frac{1}{2}\left(q_1^2 + q_2^2 + q_3^2 + q_4^2\right), \qquad M = q_1 p_2 - q_2 p_1 + q_3 p_4 - q_4 p_3. \tag{25}$$

Integrating $E(z)$, $I(z)$ and $N(z)$ over the spatial domain with periodic boundary conditions [14,15] lead to global conservation of energy, momentum and norm

$$\frac{\mathrm{d}}{\mathrm{d}t}\mathcal{E}(z) = 0, \qquad \frac{\mathrm{d}}{\mathrm{d}t}\mathcal{I}(z) = 0, \qquad \frac{\mathrm{d}}{\mathrm{d}t}\mathcal{N}(z) = 0, \tag{26}$$

where $\mathcal{E}(z) = \int_0^L E(z)\,\mathrm{d}x$, $\mathcal{I}(z) = \int_0^L I(z)\,\mathrm{d}x$, $\mathcal{N}(z) = \int_0^L N(z)\,\mathrm{d}x$. Under periodic boundary conditions we have also mass conservation:

$$C_1 = \int_0^L |\psi_1|^2\,\mathrm{d}x, \qquad C_2 = \int_0^L |\psi_2|^2\,\mathrm{d}x. \tag{27}$$

We notice that $2\mathcal{N} = C_1 + C_2$, hence the conserved quantities $\mathcal{N}$, C_1 and C_2 are dependent.

3.2. Multi-symplectic discretization of the CNLS system

Bridges and Reich introduced in [21], the concept of multi-symplectic integration. One of the most popular multi-symplectic integrator is the Preissman scheme, which corresponds to mid-point discretization in space and time variables. The Preissman scheme for (18) is given

$$\mathbf{M}\frac{z_{m+1/2}^{n+1} - z_{m+1/2}^{n}}{\Delta t} + \mathbf{K}\frac{z_{m+1}^{n+1/2} - z_{m}^{n+1/2}}{\Delta x} = \nabla_z S\left(z_{m+1/2}^{n+1/2}\right),$$

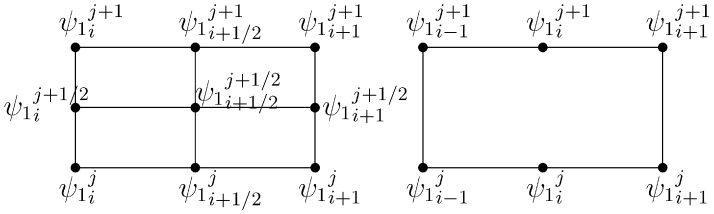

Fig. 1. Preissman scheme (left) and six-point difference scheme (right) for the CNLS equation.

with

$$z_{m+1/2}^{n}=\frac{z_m^n+z_{m+1}^n}{2},\qquad z_m^{n+1/2}=\frac{z_m^n+z_m^{n+1}}{2},\qquad \hat{z}=z_{m+1/2}^{n+1/2}=\frac{z_m^n+z_{m+1}^n+z_m^{n+1}+z_{m+1}^{n+1}}{4},$$

where Δt, Δx are time and space steps, z_m^n is an approximation to $z(n\Delta t, m\Delta x)$. The Preissman scheme preserves the discrete form of the multi-symplecticity (19) exactly and is second-order accurate in the time and space variables [21].

The Preissman scheme is one of the most successful multi-symplectic integrators and is applied for modeling wave propagation (e.g., for the KdV equation [23,24], for Klein–Gordon equation [25], particularly to the NLS equation [9,14,15,26]).

The multi-symplectic Preissman scheme for the CNLS equation is given as

$$\begin{aligned}
&\frac{q_2{}_{m+1/2}^{n+1}-q_2{}_{m+1/2}^{n}}{\Delta t}+\frac{p_1{}_{m+1}^{n+1/2}-p_1{}_{m}^{n+1/2}}{\Delta x}=\big(\sigma_1\big((\hat{q}_1)^2+(\hat{q}_2)^2\big)+v\big((\hat{q}_3)^2+(\hat{q}_4)^2\big)\big)\hat{q}_1,\\
&-\frac{q_1{}_{m+1/2}^{n+1}-q_1{}_{m+1/2}^{n}}{\Delta t}-\frac{p_2{}_{m+1}^{n+1/2}-p_2{}_{m}^{n+1/2}}{\Delta x}=\big(\sigma_1\big((\hat{q}_1)^2+(\hat{q}_2)^2\big)+v\big((\hat{q}_3)^2+(\hat{q}_4)^2\big)\big)\hat{q}_2,\\
&\frac{q_4{}_{m+1/2}^{n+1}-q_4{}_{m+1/2}^{n}}{\Delta t}+\frac{p_3{}_{m+1}^{n+1/2}-p_3{}_{m}^{n+1/2}}{\Delta x}=\big(\sigma_2\big((\hat{q}_3)^2+(\hat{q}_4)^2\big)+v\big((\hat{q}_1)^2+(\hat{q}_2)^2\big)\big)\hat{q}_3,\\
&-\frac{q_3{}_{m+1/2}^{n+1}-q_3{}_{m+1/2}^{n}}{\Delta t}-\frac{p_4{}_{m+1}^{n+1/2}-p_4{}_{m}^{n+1/2}}{\Delta x}=\big(\sigma_2\big((\hat{q}_3)^2+(\hat{q}_4)^2\big)+v\big((\hat{q}_1)^2+(\hat{q}_2)^2\big)\big)\hat{q}_4,\\
&\frac{q_1{}_{m+1/2}^{n+1/2}-q_1{}_{m}^{n+1/2}}{\Delta x}=\frac{\hat{p}_1}{\alpha_1},\qquad \frac{q_2{}_{m+1/2}^{n+1/2}-q_2{}_{m}^{n+1/2}}{\Delta x}=\frac{\hat{p}_2}{\alpha_1},\\
&\frac{q_3{}_{m+1/2}^{n+1/2}-q_3{}_{m}^{n+1/2}}{\Delta x}=\frac{\hat{p}_3}{\alpha_2},\qquad \frac{q_4{}_{m+1/2}^{n+1/2}-q_4{}_{m}^{n+1/2}}{\Delta x}=\frac{\hat{p}_4}{\alpha_2}.
\end{aligned}$$

where $\hat{q}_1=q_1{}_{m+1/2}^{n+1/2}$, etc. However, for the numerical solution of the CNLS system (1) we need only the values of ψ_1 and ψ_2. Therefore from the equation above the canonical momenta p_j can be eliminated and one obtains a new scheme. The multi-symplectic six-point scheme (MS6) can be written explicitly as

$$\begin{aligned}
&i\frac{(\psi_1{}_{m-1}^{n+1}+2\psi_1{}_{m}^{n+1}+\psi_1{}_{m+1}^{n+1})-(\psi_1{}_{m-1}^{n}+2\psi_1{}_{m}^{n}+\psi_1{}_{m+1}^{n})}{4\Delta t}\\
&\quad+\alpha_1\frac{(\psi_1{}_{m-1}^{n+1}-2\psi_1{}_{m}^{n+1}+\psi_1{}_{m+1}^{n+1})+(\psi_1{}_{m-1}^{n}-2\psi_1{}_{m}^{n}+\psi_1{}_{m+1}^{n})}{2\Delta x^2}\\
&\quad+\big(\sigma_1|\tilde{\psi}_1|^2+v|\tilde{\psi}_2|^2\big)\tilde{\psi}_1+\big(\sigma_1|\hat{\psi}_1|^2+v|\hat{\psi}_2|^2\big)\hat{\psi}_1=0, \qquad (28)\\
&i\frac{(\psi_2{}_{m-1}^{n+1}+2\psi_2{}_{m}^{n+1}+\psi_2{}_{m+1}^{n+1})-(\psi_2{}_{m-1}^{n}+2\psi_2{}_{m}^{n}+\psi_2{}_{m+1}^{n})}{4\Delta t}\\
&\quad+\alpha_2\frac{(\psi_2{}_{m-1}^{n+1}-2\psi_2{}_{m}^{n+1}+\psi_2{}_{m+1}^{n+1})+(\psi_2{}_{m-1}^{n}-2\psi_2{}_{m}^{n}+\psi_2{}_{m+1}^{n})}{2\Delta x^2}\\
&\quad+\big(v|\tilde{\psi}_1|^2+\sigma_2|\tilde{\psi}_2|^2\big)\tilde{\psi}_2+\big(v|\hat{\psi}_1|^2+\sigma_2|\hat{\psi}_2|^2\big)\hat{\psi}_2=0, \qquad (29)
\end{aligned}$$

where $\tilde{\psi}=\psi_{m-1/2}^{n+1/2}$ and $\hat{\psi}=\psi_{m+1/2}^{n+1/2}$. We remark that the scheme couples two time levels in contrast to Preissman scheme, which involves three time levels (see Fig. 1). For the single NLS equation, the six-point difference scheme is derived in [12] and later applied to the CNLS system in [9].

When $S(z)$ is quadratic, which corresponds to the linear PDE in multi-symplectic form, using the Preissman scheme the local discrete energy and discrete momentum would be preserved exactly. For the CNLS system, only the local norm (25) which contains quadratic terms is preserved exactly. From the global invariants momentum $\mathcal{I}$ and $\mathcal{N}$ containing quadratics terms are also preserved

exactly; in numerical experiments up to machine accuracy. Otherwise the local discrete energy and momentum, global energy are not preserved exactly, but numerical results and backward error analysis show that they are very well preserved over long time [14,15,27,28]. Backward error analysis with modified equations provides more information about the behavior of the numerical solutions and preservation of modified energy and momentum conservation laws. It was shown for the NLS equation by using Preissman scheme that the modified conservation laws are satisfied to a high-order by the numerical solution in [27]. Similar results are obtained for the nonlinear wave equation and Sine–Gordon equation in [28].

In [9] the same multi-symplectic six-point scheme (28)–(29) is used for the simulation of soliton collisions of the CNLS system. Energy and norm conservation properties of the scheme are shown analytically and for the global errors numerical results are presented.

This multi-symplectic formulation characterizes the Hamiltonian PDEs more deeply than the symplectic formulation, because the multi-symplectic conservation law is completely local whereas in the symplectic formulation the symplectic form is global and its variations over the spatial domain are not reflected.

4. Numerical results

In this section, we will present numerical results for the symplectic splitting method (SPL) (17) and six-point integrator (MS6) (28)–(29). The accuracy of both integrators are tested by looking at their conservation properties of energy, momentum and norm.

We consider the discrete nonlinear Hamiltonian (11) and the semi-discretized nonlinear subproblem (14). We define the discrete energy density (see p. 328 in [16])

$$E_m = \frac{1}{4}\left(\sigma_1\left(q_{1_m}^2 + q_{2_m}^2\right)^2 + \sigma_2\left(q_{3_m}^2 + q_{4_m}^2\right)^2\right) + V(q_m),$$

and find

$$\begin{aligned}\frac{\mathrm{d}}{\mathrm{d}t}E_m &= \sigma_1\left(q_{1_m}^2 + q_{1_m}^2\right)\left(q_{1m}\dot{q}_{1m} + q_{2m}\dot{q}_{2m}\right) + \sigma_2\left(q_{3_m}^2 + q_{4_m}^2\right)\left(q_{3_m}\dot{q}_{3_m} + q_{4_m}\dot{q}_{4_m}\right)\\ &\quad + v\left(q_{1m}\dot{q}_{1m} + q_{2m}\dot{q}_{2m}\right)\left(q_{3_m}^2 + q_{4_m}^2\right) + v\left(q_{1_m}^2 + q_{2_m}^2\right)\left(q_{3m}\dot{q}_{3m} + q_{4m}\dot{q}_{4m}\right) = 0\end{aligned}$$

which shows that the energy is preserved for the semi-discretized nonlinear subproblem (14). Now we consider the discrete linear Hamiltonian (10) and the semi-discretized linear subproblem (12). We define the discrete energy density

$$E_m = -\frac{\alpha_1}{2}\left[\left(\frac{q_{1m+1}-q_{1m}}{\Delta x}\right)^2 + \left(\frac{q_{2m+1}-q_{2m}}{\Delta x}\right)^2\right] - \frac{\alpha_2}{2}\left[\left(\frac{q_{3m+1}-q_{3m}}{\Delta x}\right)^2 + \left(\frac{q_{4m+1}-q_{4m}}{\Delta x}\right)^2\right],$$

and find

$$\begin{aligned}\frac{\mathrm{d}}{\mathrm{d}t}E_m &= -\alpha_1\left[\left(\frac{q_{1m+1}-q_{1m}}{\Delta x}\right)\left(\frac{\dot{q}_{1m+1}-\dot{q}_{1m}}{\Delta x}\right) + \left(\frac{q_{2m+1}-q_{2m}}{\Delta x}\right)\left(\frac{\dot{q}_{2m+1}-\dot{q}_{2m}}{\Delta x}\right)\right]\\ &\quad - \alpha_2\left[\left(\frac{q_{3m+1}-q_{3m}}{\Delta x}\right)\left(\frac{\dot{q}_{3m+1}-\dot{q}_{3m}}{\Delta x}\right) + \left(\frac{q_{4m+1}-q_{4m}}{\Delta x}\right)\left(\frac{\dot{q}_{4m+1}-\dot{q}_{4m}}{\Delta x}\right)\right].\end{aligned}$$

Here we see that the difference $(q_{j_{m+1}} - q_{j_m})/\Delta x$ is forward difference approximation to the canonical momenta p_j, $j = 1, \ldots, 4$, in (21). Thus substituting $p_{j_m} = (q_{j_{m+1}} - q_{j_m})/\Delta x$, $j = 1, \ldots, 4$, in the previous equality, we have obtained the semi-discrete energy conservation law

$$\frac{\mathrm{d}}{\mathrm{d}t}E_m + \frac{F_{m+1} - F_m}{\Delta x},$$

where

$$F_m = p_{1m}\dot{q}_{1m} + p_{2m}\dot{q}_{2m} + p_{3m}\dot{q}_{3m} + p_{4m}\dot{q}_{4m}.$$

Applying the implicit midpoint rule in time, we can use as residual

$$R_{se} = \frac{E_m^{n+1} - E_m^n}{\Delta t} + \frac{F_{m+1}^{n+1/2} - F_m^{n+1/2}}{\Delta x} \tag{30}$$

of a fully discretized local energy conservation of the symplectic splitting integrator (17) (see [12]) with

$$\begin{aligned}E_m^n &= \frac{\sigma_1}{4}\left(\left(q_{1_m}^n\right)^2 + \left(q_{2_m}^n\right)^2\right)^2 + \frac{\sigma_2}{4}\left(\left(q_{3_m}^n\right)^2 + \left(q_{4_m}^n\right)^2\right)^2 - \frac{1}{2\alpha_1}\left(\left(p_{1_m}^n\right)^2 + \left(p_{2_m}^n\right)^2\right)\\ &\quad - \frac{1}{2\alpha_2}\left(\left(p_{3_m}^n\right)^2 + \left(p_{4_m}^n\right)^2\right) + \frac{v}{2}\left(\left(q_{1_m}^n\right)^2 + \left(q_{2_m}^n\right)^2\right)\left(\left(q_{3_m}^n\right)^2 + \left(q_{4_m}^n\right)^2\right)\end{aligned}$$

and

$$F_m^{n+1/2} = p_{1_m}^{n+1/2}\left(\frac{q_{1_m}^{n+1} - q_{1_m}^{n}}{\Delta t}\right) + p_{2_m}^{n+1/2}\left(\frac{q_{2_m}^{n+1} - q_{2_m}^{n}}{\Delta t}\right) + p_{3_m}^{n+1/2}\left(\frac{q_{3_m}^{n+1} - q_{3_m}^{n}}{\Delta t}\right) + p_{4_m}^{n+1/2}\left(\frac{q_{4_m}^{n+1} - q_{4_m}^{n}}{\Delta t}\right).$$

For the multi-symplectic six-point integrator the residual in the energy conservation is given by (see, for example, [15])

$$R_{ms} = \frac{E_{m+1/2}^{n+1} - E_{m+1/2}^{n}}{\Delta t} + \frac{F_{m+1}^{n+1/2} - F_{m}^{n+1/2}}{\Delta x}. \tag{31}$$

The residuals in the momentum and norm conservation laws are defined analogously for both integrators.

The global energy error for both integrators is given by

$$GE = \Delta x \sum_{j=1}^{N} \left(E_j^n - E^0\right),$$

where E^0 is the initial energy. Global error in momentum and norm conservation laws can be define analogously.

We notice that for the invariant (31), we need the terms p_i^n which have been turn up in the elimination process of the Preissman scheme. The canonical momenta p_j, $j = 1, \ldots, 4$, in (21) are approximated by using the forward difference and implicit midpoint rule for the SPL and MS6, respectively, to obtain the discrete terms $p_{j_m}^n$.

4.1. Symmetric initial conditions

As symmetric initial conditions two initially perturbed periodic waves

$$\psi_1(x,0) = \psi_{10}\left(1 - \epsilon\cos(lx)\right), \qquad \psi_2(x,0) = \psi_{20}\left(1 - \epsilon\cos l(x+\theta)\right) \tag{32}$$

are used, where the parameter $\epsilon \ll 1$ describes the strength of the perturbation, l is the wave number of the perturbation and θ represents the initial phase difference between two perturbations [6]. The phase difference θ is set to zero in [5]. In both papers, the wave numbers k_1 and k_2 have been taken to zero only for the purpose of showing the evolution of the solution clearly. In the numerical experiments we choose $l = 1/2$ and $\epsilon = 0.1$. As boundary conditions, periodic boundary conditions $u(x,t) = u(x+L,t)$ with $L = 8\pi$ are used. The initial conditions (32) are symmetric, i.e.

$$\psi_1(x,0) = \psi_1(L-x,0), \qquad \psi_2(x,0) = \psi_2(L-x,0).$$

When the initial conditions are symmetric, the solutions $\psi_1(x,t)$ and $\psi_2(x,t)$ are symmetric too (see [10]).

The time initial was taken as $T = [0, 100]$. For both integrators we have taken $\Delta x = L/128$ and as time step size $\Delta t = 0.05$. The nonlinear equations arising in both integrators are solved using the simplified Newton method at each time step with an error tolerance 10^{-5}.

From the linear stability analysis [5], it follows that the plane wave solution is linearly stable if the wave number of perturbation l is greater than the critical value l_c depending on the initial amplitudes ψ_{10} and ψ_{20} of the unperturbed periodic waves, otherwise it is unstable.

In the following we consider three different cases corresponding to elliptic, linear and circular polarizations as in [5,6].

4.1.1. Elliptic polarization ($v = 1$)

This is the integrable case that Manakov [1] studied. The critical value for the elliptic polarization is given by $l_c = \sqrt{2(\psi_{10}^2 + \psi_{20}^2)}$. For the choice of $\psi_{10} = \psi_{20} = 0.5$, $l_c = 1$, $l = 0.5$ which implies that the plane wave is unstable.

Fig. 2 provides the results with $\psi_{10} = \psi_{20} = 0.5$ and $\theta = 0$. We see that, within that length there are two peaks which is called as two-hump state and the amplitude of ψ_1 and ψ_2 undergoes oscillations between the near-uniform state and the two-hump state as in the Hopscotch method [6] which is basically a Fermi–Pasta–Ulam recurrence phenomenon [29].

Fig. 3 shows the errors in local energy (30)–(31) and momentum conservation laws, for MS6 and SPL integrators. We see that the local energy, momentum and the norm are well preserved for both integrators and they do not grow with time. But the data in case of MS6 is noisy; a chekerboard instability arises. The errors are concentrated in the regions of the solutions where there are two peaks.

In Fig. 4 global errors of energy, momentum and norm (26) are plotted. Momentum and norm are preserved up to the machine accuracy for MS6 and SPL because both are quadratic invariants [10]. The global errors in the energy are almost the same for MS6 and SPL.

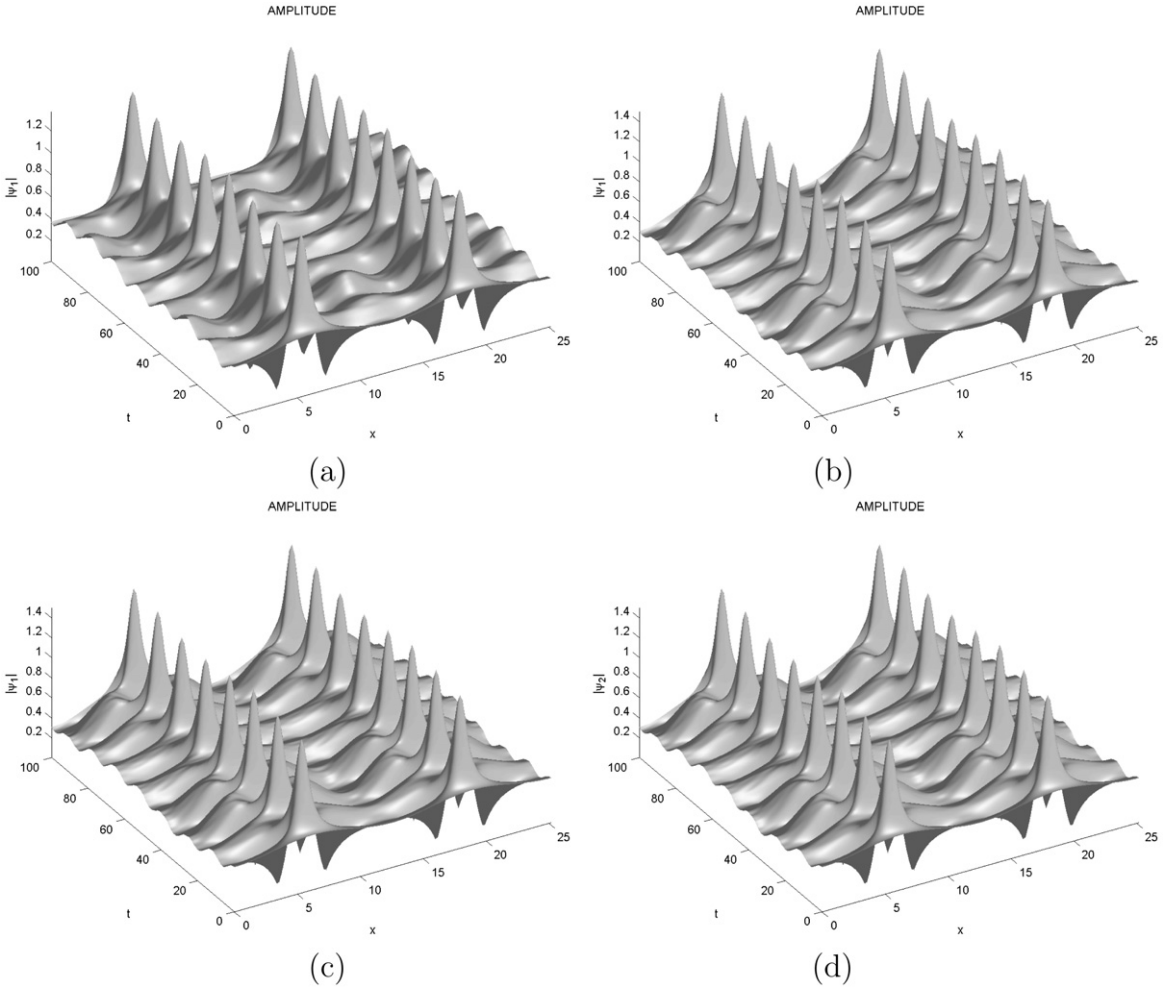

Fig. 2. Elliptic polarization, $v = 1$: Destabilized wave solutions with $\psi_{10} = 0.5$, $\psi_2 10 = 0.5$, $\epsilon = 0.1$, $\theta = 0$. Left plots: surface of $|\psi_1|$. Right plots: surface of $|\psi_2|$. (a) and (b) for MS6, (c) and (d) for SPL.

4.1.2. Linear polarization ($e = 2/3$)

This is an non-integrable case. The critical value

$$l_c = \sqrt{\psi_{10}^2 + \psi_{20}^2 + \sqrt{\left(\psi_{10}^2 + \psi_{20}^2\right) - \frac{20}{9}\psi_{10}^2\psi_{20}^2}}$$

which is $l_c = 0.91$ for $\psi_{10} = \psi_{20} = 0.5$. Again the plane waves are unstable for $l = 0.5$.

Figs. 5(a), (b) and 6(a), (b) show that the initial phase difference in $\psi_2(x, 0)$ effects the evolution of $\psi_1(x, t)$. From these figures we see that, the spatial location of peaks in $|\psi_1(x, t)|$ is affected by those in $|\psi_2(x, t)|$. We also notice that, within the introduction of a phase difference between the initial conditions, the period of oscillation increases. To see this effect one can compare Figs. 5 and 6.

On the other hand, as for the Hopscotch method [6], a phase difference between the perturbations has no effect on the spatial locations of peaks of ψ_1 and on the periodicity of the evolution of ψ_1. Figs. 5(c) and 6(c) shows the local energy errors. From Figs. 5 and 6 one can see that the errors for the energy remain bounded. The errors are concentrated in the region where there are two peaks as for the elliptic polarization. We see that within an introduction of a phase difference, the local energy error in MS6 increased whereas in the SPL it remains almost same. The local and global errors for the other invariants are almost same as in the case of the elliptic polarization, which are not shown here.

4.1.3. Circular polarization ($e = 2$)

In nonlinear optics, this is the circular polarization mode case. This case is also nonintegrable. The interaction between perturbed periodic waves is very strong since the wave–wave interaction coefficient v is two times the dispersion coefficients $\alpha_1 = \alpha_2 = 1$.

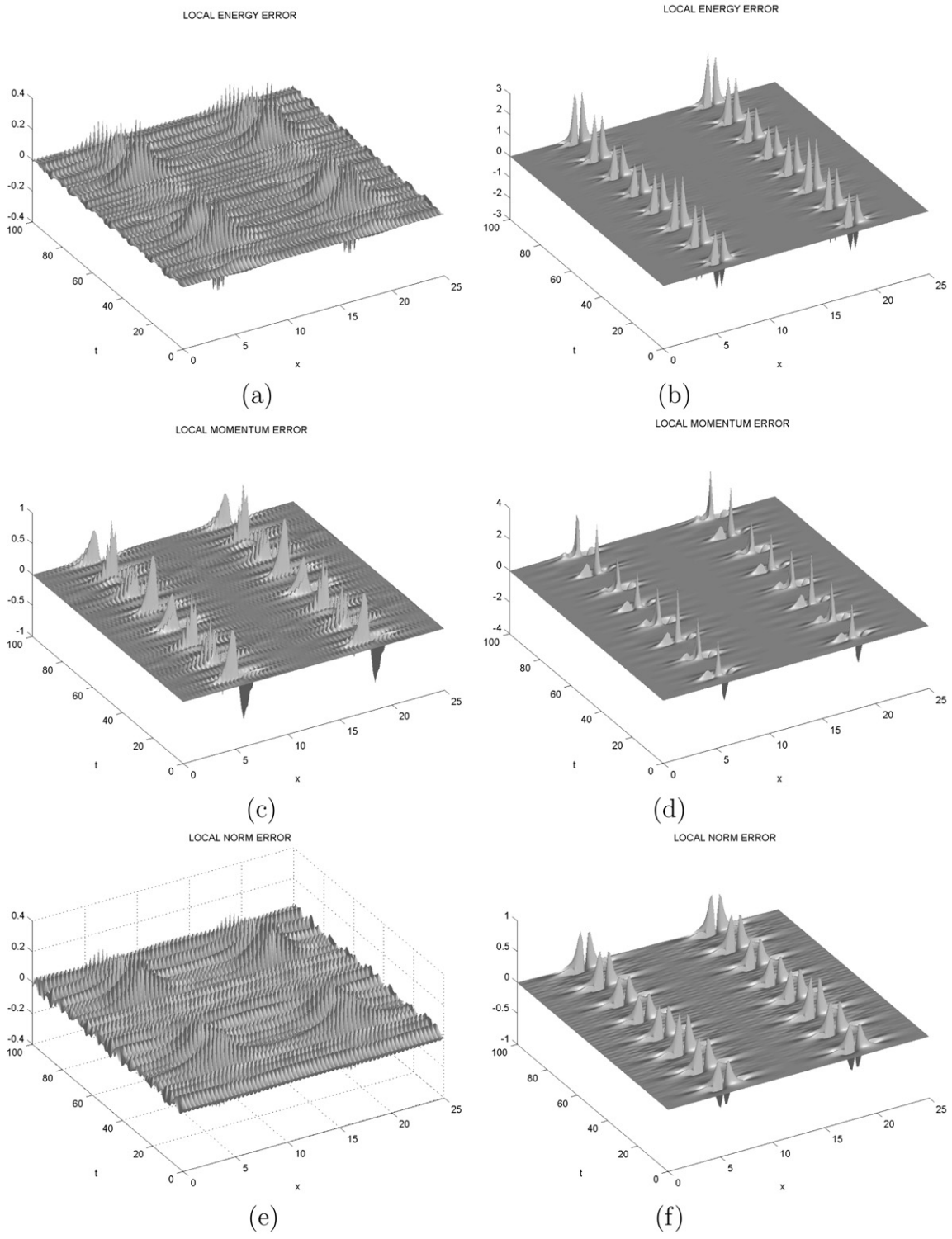

Fig. 3. Elliptic polarization, $v = 1$: Local errors for destabilized wave solutions with $\psi_{10} = 0.5$, $\psi_{20} = 0.5$, $\epsilon = 0.1$, $\theta = 0$. Left plots for MS6. Right plots for SPL.

The critical perturbation wave number is

$$l_c = \sqrt{\psi_{10}^2 + \psi_{20}^2 + \sqrt{\left(\psi_{10}^2 + \psi_{20}^2\right)^2 + 12\psi_{10}^2\psi_{20}^2}}.$$

For $\psi_{10} = \psi_{20} = 0.5$, $l_c = 1.23$ which is larger than $l = 0.5$, the plane waves are again unstable.

First we consider mass conservation (27), which is a quadratic invariant. For comparison our results with those in [6] obtained by the Hopscotch method, we consider three different cases

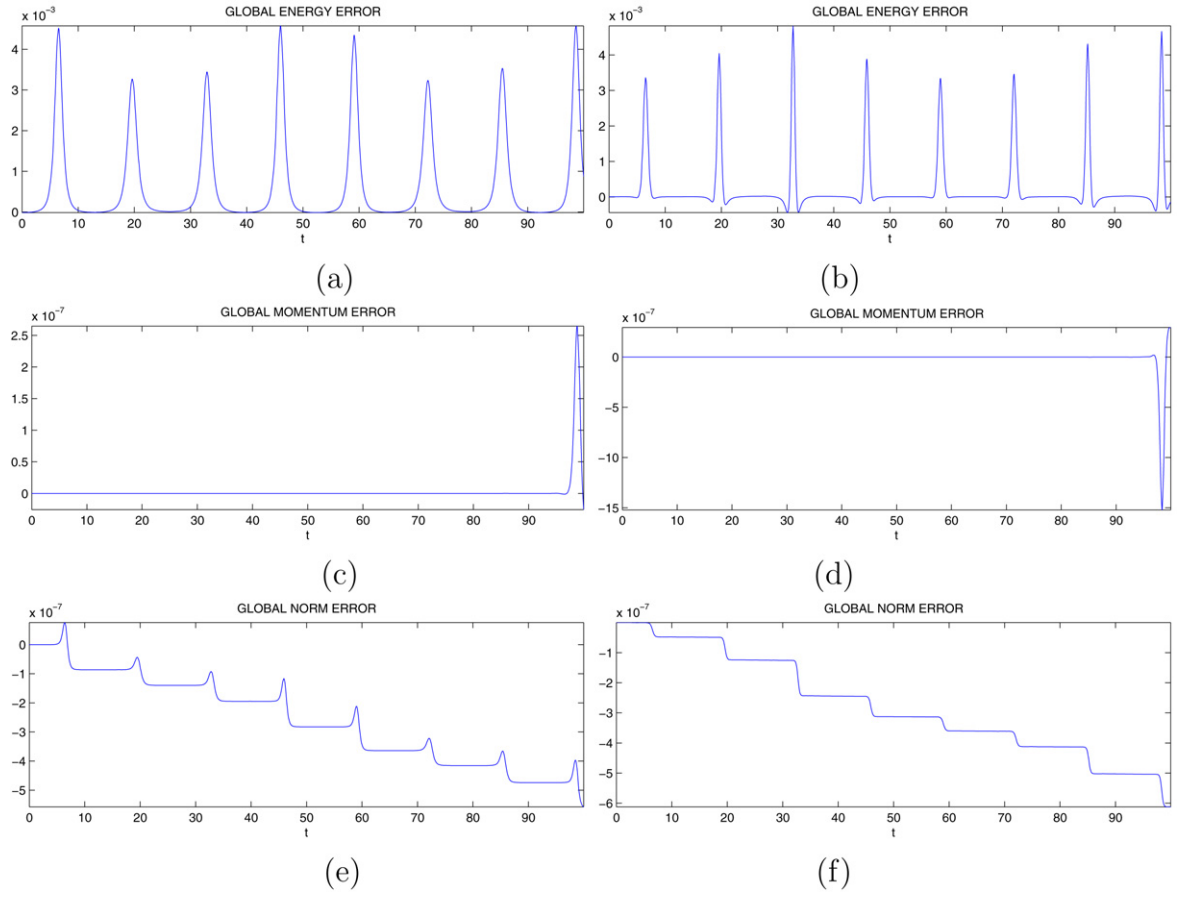

Fig. 4. Elliptic polarization, $v = 1$: Global errors for destabilized wave solutions with $\psi_{10} = 0.5$, $\psi_{20} = 0.5$, $\epsilon = 0.1$, $\theta = 0$. Left plots for MS6. Right plots for SPL.

Table 1
Errors in mass conservation for circular polarization

		(a)		(b)		(c)	
		$C_1(\psi_1)$	$C_2(\psi_2)$	$C_1(\psi_1)$	$C_2(\psi_2)$	$C_1(\psi_1)$	$C_2(\psi_2)$
MS6	$t = 50$	0.6E–2	0.6E–2	0.5E–2	0.5E–2	0.6E–2	0.5E–2
	100	3.6E–2	3.6E–2	7.7E–2	7.7E–2	1.9E–2	0.3E–2
SPL	$t = 50$	0.1E–7	0.1E–7	6.7E–7	6.7E–7	0.2E–7	0.3E–7
	100	0.2E–7	0.2E–7	0.1E–7	0.1E–7	0.5E–7	0.8E–7

(a) $\psi_{10} = 0.5$, $\psi_{20} = 0.5$, $\theta = 0$,
(b) $\psi_{10} = 0.5$, $\psi_{20} = 0.5$, $\theta = 3\pi/2$,
(c) $\psi_{10} = 0.78$, $\psi_{20} = 0.2$, $\theta = 0$.

The integrals (27) are approximated by the trapezoidal rule in Table 1. They agree for the MS6 up to two first digits with the exact values as for the Hopscotch method [6]. We notice that SPL gives more accurate results than the Hopscotch method and MS6.

The Hopscotch methods uses alternatively explicit and implicit Euler method over two time steps. Therefore it can be interpreted as first-order symplectic Euler method for the semi-discretized Hamiltonian system (9) over two time steps. Hopscotch method is conditionally stable, i.e. for some time step sizes Δt it can lead to unstable solutions [30].

From Fig. 7 we can see, when the initial amplitudes are equal $\psi_{10} = \psi_{20} = 0.5$ and with no phase difference initially, the evolution for the circular polarization is more complex than the elliptic and linear polarization cases. The results obtained using MS6 integrators show that one peak splits into two peaks and two peaks emerge again. This phenomenon repeats itself throughout the evolution. The same results were obtained in the Hopscotch method. However, the results obtained using the SPL integrator show that after a period of time the separated peaks coupled together, remain stationary and oscillating in their strength. The local errors in energy conservation for the MS6 scheme grow in time. But this growth is less than for the SPL scheme which shows a chaotic behavior in long time dynamics.

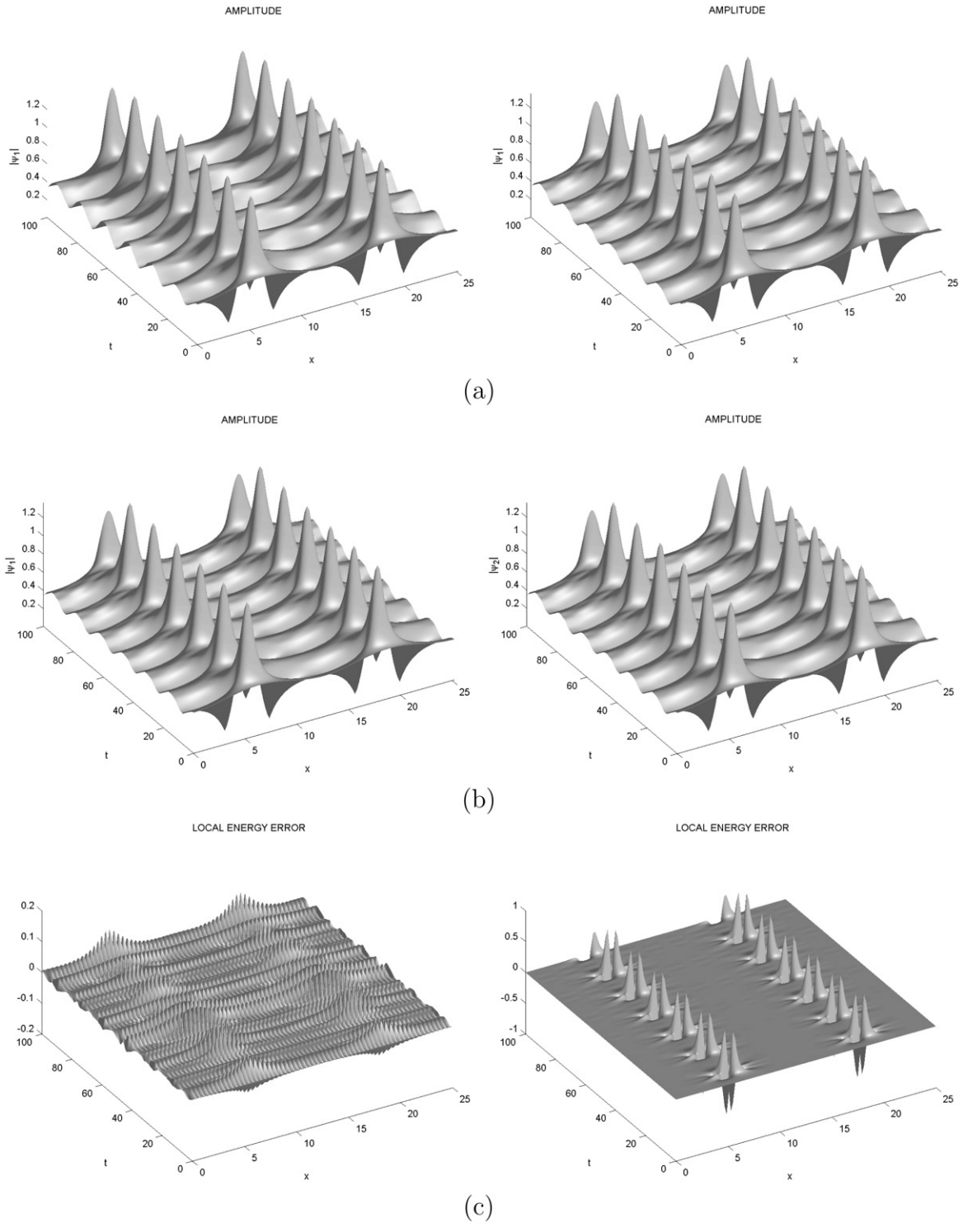

Fig. 5. Linear polarization, $v = 2/3$: Destabilized wave solutions with $\psi_{10} = 0.5$, $\psi_{20} = 0.5$, $\epsilon = 0.1$, $\theta = 0$. (a) and (b) Surfaces of $|\psi_1|$ and $|\psi_2|$: (a) For MS6, (b) for SPL. (c) Local energy errors: left plot for MS6; right plot for SPL.

4.2. Nonsymmetric initial conditions

We integrate now the CNLS (1) with the unsymmetric initial conditions

$$\psi_1(x,0) = \sqrt{\frac{2\zeta}{1+e}}\,\operatorname{sech}\left(\sqrt{2\zeta}\,x\right)\exp i\left((\rho-\delta)(x+20)\right),$$

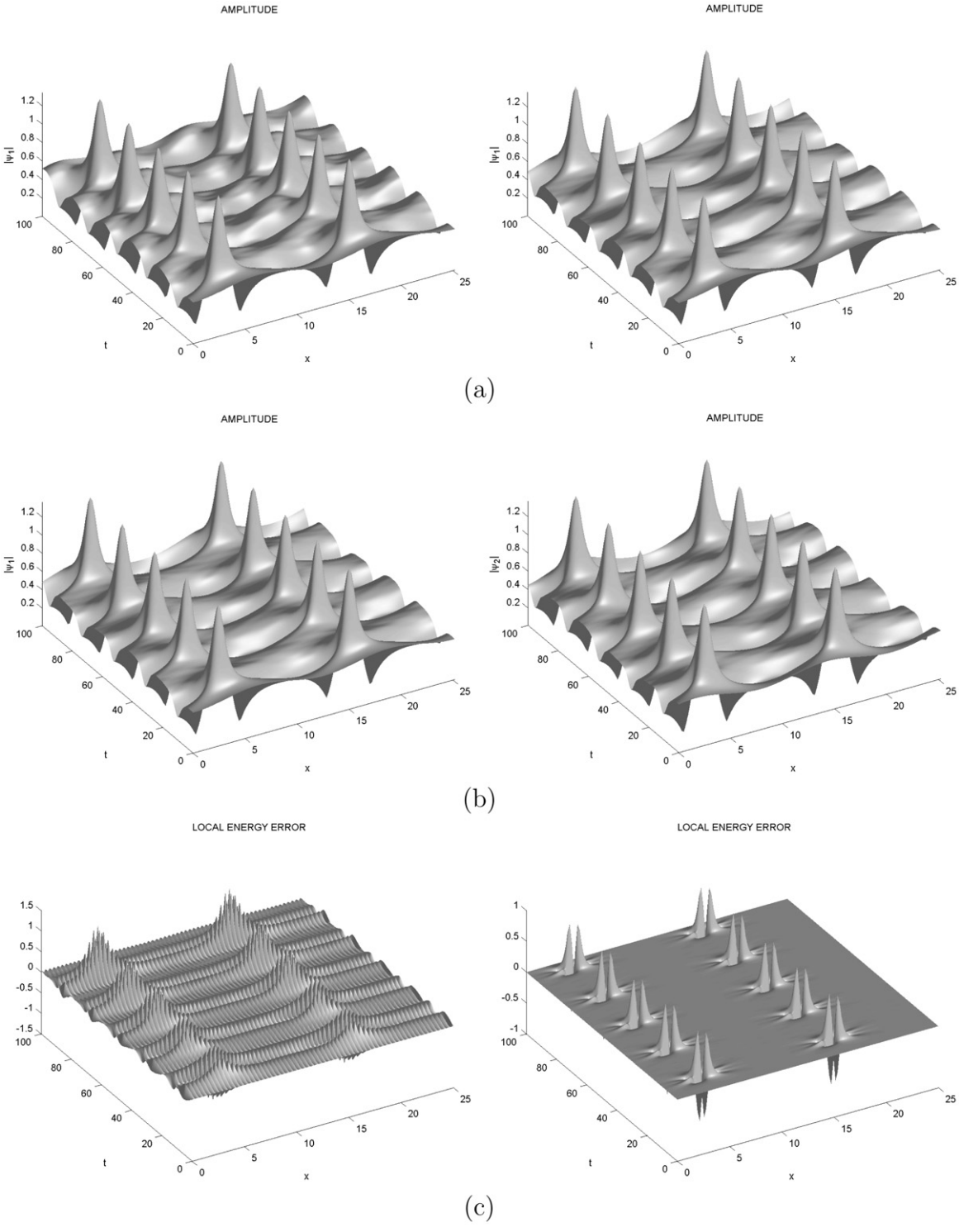

Fig. 6. Linear polarization, $v = 2/3$: Destabilized wave solutions with $\psi_{10} = 0.5$, $\psi_{20} = 0.5$, $\epsilon = 0.1$, $\theta = 3\pi/2$. (a) and (b) Surfaces of $|\psi_1|$ and $|\psi_2|$: (a) For MS6, (b) for SPL. (c) Local energy errors: left plot for MS6; right plot for SPL.

$$\psi_2(x,0) = \sqrt{\frac{2\zeta}{1+e}}\,\operatorname{sech}\left(\sqrt{2\zeta}x\right)\exp i\left((\rho+\delta)(x+20)\right),$$

where ζ, e and v are real constants [31]. This solution represents a solitary wave initially at $x = -20$. We compute the solitary wave solution for $\alpha_1 = \alpha_2 = 0.5$, $\sigma_1 = \sigma_2 = 1$ and $v = 2$ with $\rho = 1.0$ and $\zeta = 1.0$ on the interval $-40 \leqslant x \leqslant 40$. The spatial domain have been chosen large enough so that the boundaries do no effect the solitary wave propagation.

Fig. 8 shows that the evolution of a single soliton is well simulated by MS6 and SPL. From the figure we see that the single soliton is moving to the right with the velocity $v = 2$ for different times as in [31]. We notice that the errors in global energy

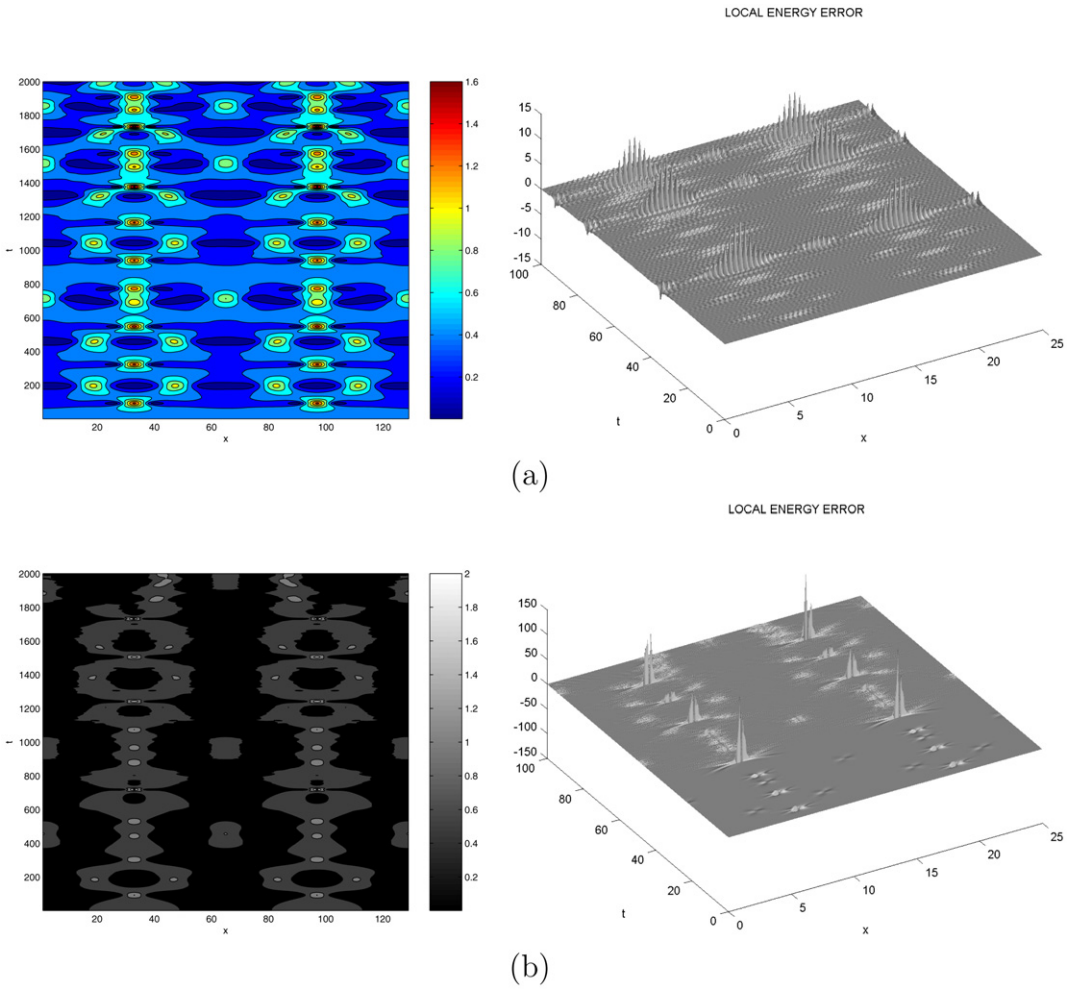

Fig. 7. Circular polarization, $v = 2$: Destabilized wave solutions $\psi_{10} = 0.5$, $\psi_{20} = 0.5$, $\epsilon = 0.1$, $\theta = 0$. (a) For MS6; Left plot: Contour plot of wave $|\psi_1|$, right plot: Local energy error. (b) For SPL; Left plot: Contour plot of wave $|\psi_1|$, right plot: Local energy error.

and momentum are bounded, whereas in errors of global norm are increasing similarly to the symmetric initial conditions given in Fig. 4. The global energy is also well preserved as in case of symmetric initial conditions. We have discretized the odd derivatives in the momentum using pseudo-spectral approximation like in [10]. The errors in the momentum are increasing with time like in [10] where the single nonlinear Schrödinger equation was considered. But the errors in the momentum are almost negligible compared to the errors in energy and norm.

Our results differ from those in [10] where for a single nonlinear Schrödinger equation with nonsymmetric initial conditions, the momentum errors are increasing over time. We have to mention that in [10] the semi-discretized Hamiltonian system (9) was integrated using the standard symplectic mid-point rule, whereas we have used a symplectic splitting composition method based on the mid-point rule.

As a summary we can state that the qualitative behavior of the numerical solutions obtained here are similar to those in [5,6,10]. In addition to this, their accuracy can be controlled by looking at the conservation properties of the energy, momentum and norm, which were not displayed in [5,6], because both methods used there are not structure-preserving.

4.3. Computational efficiency and higher-order generalizations

Both methods require solution of $4N \times 4N$ linear systems of equations which results from the simplified Newton method at each time step. MS6 requires approximately two times less computing time than SPL, because the SPL requires two nonlinear system of equations due to composition (17).

Higher-order symplectic methods are based on the formula (17). For example, the fourth-order composition method can be given as (see, for example, [18,20])

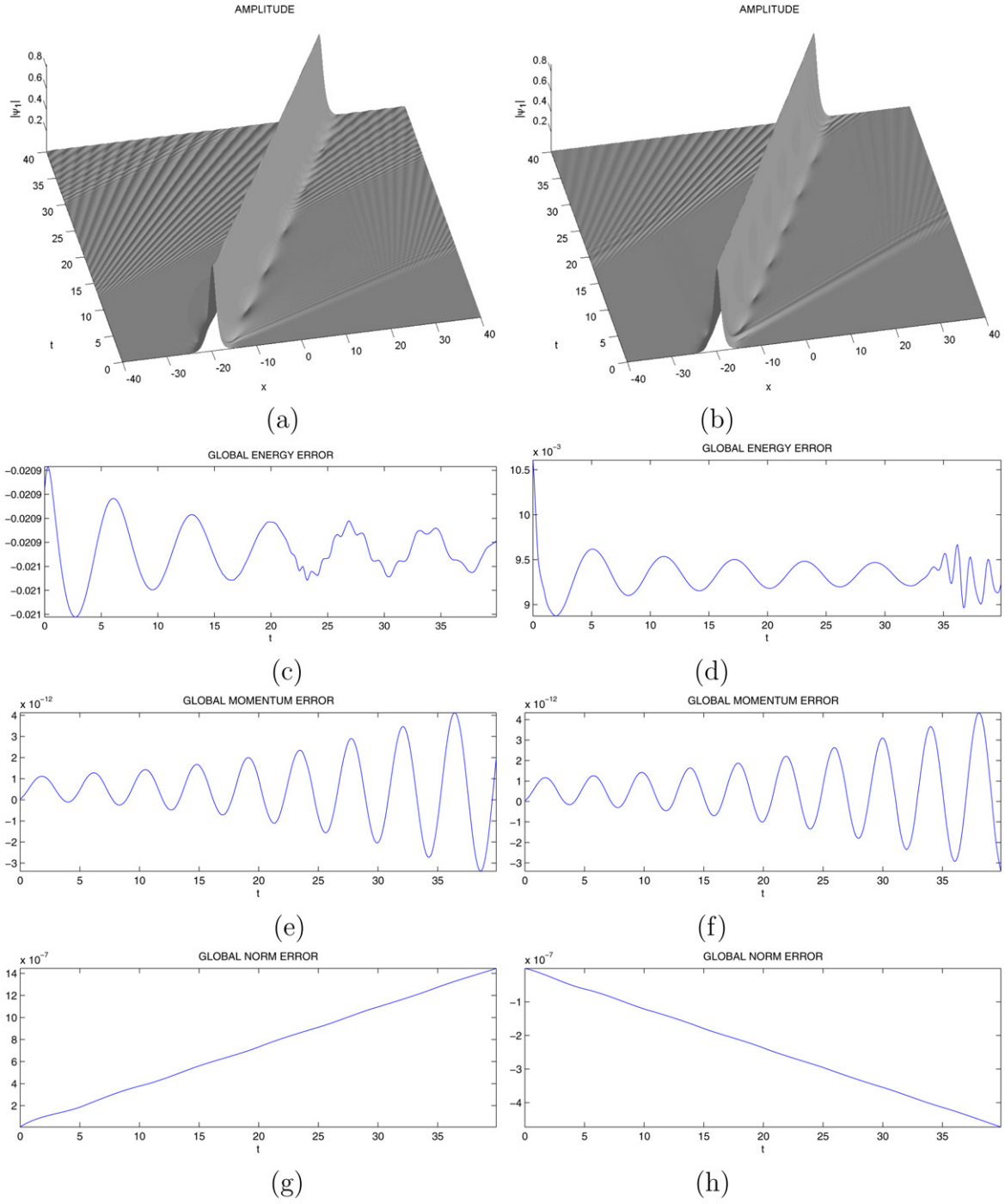

Fig. 8. Circular polarization: One soliton solution with $v = 2$. Evolution of the wave ψ_1 and global errors. Left plots for MS6. Right plots for SPL.

$$\varphi_4(\Delta t) = \varphi_2(\omega\Delta t)\varphi_2\big((1-2\omega)\Delta t\big)\varphi_2(\omega\Delta t),$$

where $\omega = (2 + 2^{1/3} + 2^{-1/3})/3$. The fourth-order composition method requires three times more computing time than the second-order one.

Gauss–Legendre collocation methods are the higher-order generalization of the Preissman scheme, which were developed as multi-symplectic integrators in [32]. Gauss–Legendre methods require coupled system of nonlinear equations for computing the stage vectors. Multi-symplectic integrators based on Gauss–Legendre Runge–Kutta methods require to solve a system of s^2N equations. For higher-order schemes they can be computationally more costly than the composition methods based on symplectic splitting.

5. Conclusions

In this paper, a system of coupled nonlinear Schrödinger equations with unstable periodic plane wave solutions are integrated by two special methods from the class of symplectic and multi-symplectic integrators. Both integrators preserve the energy, momentum very well in long-time. Because the mass, norm and the global momentum are quadratic invariants, they are preserved by both methods very accurately for long times. Although the multi-symplectic integrators possess a local nature, the numerical results indicate that the symplectic scheme has very similar local preservation properties as the multi-symplectic six-point scheme. The global invariants are preserved for both methods with almost the same accuracy. The local and global preservation properties of the invariants of both methods are reflected in the plane wave solution like in Fig. 8(a) and (b) which are very close to each other. Both methods are structure-preserving and the qualitative behavior of the solution can be checked by looking at the local and global conservation of the invariants like energy, momentum, norm and mass. Therefore they are more favorable than those methods used recently for plane waves with periodic solution in [5,6].

Due to the splitting of the Hamiltonian in linear and nonlinear parts and using the composition (17) in time, the symplectic method requires more computing time than the multi-symplectic integrator. One could discretize the Hamiltonian using the central difference approximation for space derivatives to obtain a finite-dimensional Hamiltonian system and without splitting the Hamiltonian, discretize the time derivatives using a symplectic Gauss–Legendre Runge–Kutta method like in [12]. But as stated in Section 4.3, higher-order generalizations of the implicit mid-point rule, the symplectic Gauss–Legendre Runge–Kutta methods would require more computing time than the higher-order composition methods.

The residuals in the local energy are calculated for both methods using the formulas (30)–(31) which reflect the discretization in time and space. We have observed almost the same local error behavior for the local energy for the splitting method using

$$R_{se} = \frac{E_m^{n+1} - E_m^n}{\Delta t} + \frac{F_{m+1}^n - F_m^n}{\Delta x}$$

instead of using (30).

The choice of particular initial conditions like symmetric or nonsymmetric can affect the preservation of the invariants differently. This should be investigated in future more in detail.

Acknowledgements

The authors thank to the referees for their valuable comments and suggestions.

References

[1] S.V. Manakov, On the theory of two-dimensional stationary self-focusing of electromagnetic waves, Sov. Phys. JETP 38 (1974) 248.
[2] C.R. Menyuk, Stability of solitons in birefringent optical fibers, J. Opt. Soc. Amer. B 5 (1988) 392.
[3] B. Tan, Collision interactions of envelope Rossby solitons in a barometric atmosphere, J. Atmos. Sci. 53 (1996) 1604.
[4] B. Tan, S. Liu, Collision interactions of solitons in a barometric atmosphere, J. Atmos. Sci. 52 (1995) 1501.
[5] B. Tan, J.P. Boyd, Stability and long time evolution the periodic solutions of the two coupled nonlinear Schrödinger equations, Chaos Solitons Fractals 12 (2001) 721.
[6] S.C. Tsang, K.W. Chow, The evolution of periodic waves of the coupled nonlinear Schrödinger equations, Math. Comput. Simulation 66 (2004) 551.
[7] V.E. Zakharov, E.L. Schulman, To the integrability of the system of two coupled nonlinear Schrödinger equations, Physica D 4 (1982) 270.
[8] J.Q. Sun, X.Y. Gu, Z.Q. Ma, Numerical study of the soliton waves of the coupled nonlinear Schrödinger system, Physica D 196 (2004) 311.
[9] J.Q. Sun, M.Z. Qin, Multi-symplectic methods for the coupled 1D nonlinear Schrödinger system, Comput. Phys. Comm. 155 (2003) 221.
[10] B. Cano, Conserved quantities of some Hamiltonian wave equations after full discretization, Numer. Math. 103 (2006) 197.
[11] T.J. Bridges, S. Reich, Numerical methods for Hamiltonian PDEs, J. Phys. A: Math. Gen. 39 (2006) 5287.
[12] J.B. Chen, M.Z. Qin, Y.F. Tang, Symplectic and multisymplectic methods for the nonlinear Schrödinger equation, Comput. Math. Appl. 43 (2002) 1095.
[13] B.M. Herbst, F. Varadi, M.J. Ablowitz, Symplectic methods for the nonlinear Schrödinger equation, Math. Comput. Simulation 37 (1994) 353.
[14] A.L. Islas, D.A. Karpeev, C.M. Schober, Geometric integrators for the nonlinear Schrödinger equation, Comput. Phys. 173 (2001) 116.
[15] A.L. Islas, C.M. Schober, On the preservation of phase structure under multisymplectic discretization, J. Comput. Phys. 197 (2004) 585.
[16] B. Leimkuhler, S. Reich, Simulating Hamiltonian Dynamics, Cambridge University Press, 2004.
[17] E. Hairer, C. Lubich, G. Wanner, Geometric Numerical Integration Structure-Preserving Algorithms for Ordinary Differential Equations, vol. 31, Springer, New York, 2002.
[18] R.I. McLachlan, G.R.W. Quispel, Splitting methods, Acta Numer. (2002) 341.
[19] A. Rouhi, J. Wright, A new operator splitting method for the numerical solution of partial differential equations, Comput. Phys. Comm. 85 (1995) 18.
[20] G.M. Muslu, H.A. Erbay, Higher-order split-step Fourier schemes for the generalized nonlinear Schrödinger equation, Math. Comput. Simulation 67 (2005) 581.
[21] T.J. Bridges, S. Reich, Multi-symplectic integrators: numerical schemes for Hamiltonian PDEs that conserve symplecticity, Phys. Lett. A 284 (2001) 184.
[22] T.J. Bridges, T.J. Laine-Pearson, Multisymplectic relative equilibria, multiphase wavetrains, and coupled NLS equations, Stud. Appl. Math. 107 (2001) 137.
[23] U. Ascher, R. McLachlan, Multisymplectic box schemes and the Korteweg de Vries equation, Appl. Numer. Math. 48 (2004) 255.
[24] P.F. Zhao, M.Z. Qin, Multisymplectic geometry and multisymplectic Preissman scheme for the KdV equation, J. Phys. A: Math. General 33 (2000) 3613.
[25] Y.S. Wang, M.Z. Qin, Multisymplectic schemes for the nonlinear Klein–Gordon equation, Math. Comp. Modeling 36 (2002) 963.

[26] J.B. Chen, M.Z. Qin, A multisymplectic variational integrator for the nonlinear Schrödinger equation, Numer. Methods Partial Differential Equations 18 (2002) 523.
[27] A.L. Islas, C.M. Schober, Backward error analysis for multisymplectic discretizations of Hamiltonian PDEs, Math. Comput. Simulation 69 (2005) 290.
[28] B. Moore, S. Reich, Backward error analysis for multi-symplectic integration methods, Numer. Math. 95 (2003) 625.
[29] N.N. Akhmediev, Nonlinear physics—déjà vu in optics, Nature 413 (2001) 267.
[30] D. Furihata, Finite difference schemes for $\partial u/\partial t = (\partial/\partial x)^{\alpha}\delta G/\delta u$ that inherit energy conservation or dissipation property, J. Comput. Phys. 156 (1999) 181.
[31] M.S. Ismail, T.R. Taha, Numerical simulation of coupled nonlinear Schrödinger equation, Math. Comput. Simulation 56 (2001) 547.
[32] S. Reich, Multi-symplectic Runge–Kutta collocation methods for Hamiltonian wave equations, Comput. Phys. 157 (2000) 473.